Experimental and Numerical Heat Transfer Investigation of Impingement Jet Nozzle Position in Concave Double-Wall Cooling Structures

Edward Wright[1*], Abdallah Ahmed[1], Yuying Yan[1], John Maltson[2], Lynda Arisso Lopez[1]

[1]Faculty of Engineering, University of Nottingham, Nottingham NG7 2RD, United Kingdom

[2]Siemens Industrial Turbomachinery Ltd, Firth Road LN6 7AA, Lincoln, United Kingdom

*Edward Wright: Edward.Wright1@nottingham.ac.uk

ABSTRACT

In this paper, experimental and numerical study has been carried out to investigate impingement cooling with a row of five circular jets, varied between target positions on a realistic leading edge region of a gas turbine blade geometry. Experimental data is collected from a transient thermochromic liquid crystal measurement technique at the target surface. Numerical study was conducted with the geometry using commercial computational fluid dynamics software to analyse the fluid flow. The unique aims of the study are to observe the effects of variation in jet location, and those specific to realistic target and nozzle geometries. Distributions of local and average Nusselt number show that a location targeting the concave surface at 90° demonstrates an overall higher heat transfer coefficient, especially in the stagnation region, and towards the aerofoil sides, with significantly less swirl. The experiment was performed with the following parameters: distance from nozzle to target of 1.7 to 2.1 jet diameters, pitch between jets of 4.4 jet diameters, and concave target diameter of 8.0 jet diameters. The jet Reynolds number range during this test was 20,000 - 40,000. A standard flat target plate impingement test is also experimentally conducted and compared against existing literature for method validation.

Introduction

Since the advent of gas-turbine powered aircraft, and their widespread use since the mid-20th century, the design of cooled aerofoils has been much investigated [1]. Due to persistent interest for increased power, efficiency, and lifespan of both aero and industrial gas turbines since then has led to typical turbine entry temperatures (TET) doubling over this 70 year timespan. To accommodate this rapid development; a vast sum of resources have been deployed in driving the technological development of cooling mechanisms which are necessary to sustain this advancement, protecting the critical turbine stage nozzles and blade components. Significant contribution to this development has come from material science, but the majority has been from the utilisation of cooling air bled from the compressor [2]. Within industry, the initial cooling geometries developed following the Second World War, and seeing commercial use in the 1960s employed simple, cylindrical passages which used the compressors relatively cold air flow and forced convection to transfer heat from the metal aerofoil, and into the fluid which could then be expelled [3]. During the next 30 years these passages complexified and acquired features to increase the turbulence of this cooling air, therefore raising local heat transfer [4]. Towards the end of the century, new technologies such as film cooling and jet impingement began to see a rapid development and deployment, vastly increasing the TET [5].

Jet impingement particularly, is a method of cooling which allows for highly customised levels of local heat transfer, it is a technique whereby a jet of air is focussed through a nozzle, and onto a target surface where the jet then performs heat or mass transfer locally against that surface [1]. This method generates a very high coefficient of heat or mass transfer in the stagnation region and can be adapted easily to modify the resultant boundary layer properties, therefore specifically achieving desired levels of transfer [6].

Since the inception of jet impingement, much research has been conducted to maximise the heat transfer of a single impinging jet against a target surface, and to understand the nature of the jet. These studies primarily utilise the dimensionless value of Nusselt number to compare the effects of many factors; such as turbulence, turbulence intensity, jet to target distance, and the potential core of an impinging jet. Although the gas turbine application has been a major drive for research on jet impingement, development has also branched to other heat and mass transfer applications, with variations in design parameters, such as reactor boiler cooling [7], and paper drying [8].

The basis of this research is a relationship between the turbulence of a jet, and the resultant heat or mass transfer it produces. The non-dimensionalised value of Reynolds number (Re) is used to relate this turbulence, based on the jet mass flow rate, to the resultant Nusselt number. Many jet impingement studies have analysed key variables affecting heat transfer, the preponderance presenting positive trends of Nusselt number over their tested Reynolds number ranges [1].

Geers et al. [9] also investigated turbulence intensity within impinging jets, presenting measurements of both mean and fluctuating jet velocity-components, concluding that the turbulence stress field has very strong anisotropy. The study developed knowledge of the jet's potential core, wherein centreline velocity is equal to that of the nozzle exit. Particle image velocimetry results agreed with pervious researches by Cooper et al. [10] and Kataoka [11], who demonstrated the length of a turbulent circular jet core to be four to five nozzle diameters long. As the fluid exits the nozzle, the potential core is the region within the jet, where jet velocity remains constant to the nozzle exit velocity.

Due to the potential core, and subsequent development of boundary layer, the effect of jet to target spacing (H) and jet diameter (D) on heat transfer become a key consideration for jet impingement design. Huang and El-Genk [12] investigated an H/D range of 1 to 12, where the H value is measured as the distance from the jet nozzle, to the target impingement surface. The potential core is diminished as H/D increases, and therefore it is key to consider its effect on the optimisation of H/D. Maximum stagnation point Nusselt number (Nu_0) occurred at an H/D of 4.7. This research also provided correlation on the reduction of heat transfer with radial distance away from the stagnation point, as the impingement jet turns to a wall jet with developing boundary layer.

Innovation on jet impingement optimisation still continues to show promise, with recent modifications such as synthetic modification to the jet, via acoustic excitation showing increases in vortex strength, and flow control [13]. Modern additive manufacturing (AM) technology is also allowing for reviewed investigation into other techniques such as fluidic oscillators in the turbine cooling application, with potential to provide an oscillating jet of cooling air through a wide fan angle [14].

Although these jets can be utilised singularly in areas where a particularly concentrated heat transfer coefficient (HTC) is required, and investigation into this continues, for a long time researchers have also looked at their potential utilisation within a row, or an array to maximise the high heat transfer benefits seen in the stagnation region over a larger area [15]. Many studies investigating optimisation of the additional geometric variables involved with multiple jets, such as the pitch between jets relative to their diameter (p/D), and how this affects the optimisation of (H/D), alongside other geometrical variations, be these due to geometry requirements, or manufacturing constraints. When distance between subsequent jets (p) is decreased relative to the nozzle D, a more uniform target surface cooling can be achieved, but jet to jet interaction is increased, with potential detriment to the effectiveness of each individual jet [16]. Of particular interest in this paper, are the effects of a concave type target surface on the effectiveness of a row of impinging jets, specifically in applications when cooling hot end turbine aerofoil components. Within a hollow turbine blade or nozzle, the impingement geometry can be produced using traditional investment casting and machining methods, possibly utilising an insert pushed into the aerofoil base to implement the impingement jet configuration, or using more novel AM techniques [17]. With the insert, modern AM techniques, or other methods; the impingement layout is easily modified, therefore it is beneficial to decide upon the most effective design. On a flat plate, the orientation of the jet is somewhat limited to achieve optimum cooling, but with any sort of irregular concave surface; more options are presented.

An early investigation on heat transfer due to an impingement row on a concave surface was conducted to gather Nusselt number data dependant on the Jet Reynolds number and various geometric parameters [18]. With more recent investigation also further looking at the effect of the jet's inclination, either intentionally [19], or as a by-product of its relative location on the heat transfer in a symmetrical concave target section, this research was conducted to a maximum Re of 20,000 [20]. Research has been long conducted on the effects of varying an ideal nozzle's height and pitch [21], and more recently even with consideration of how that functions at low Reynolds numbers when on an approximation of a leading edge concave [22], and even more recently with a more realistic geometry [23], and at more realistic Reynolds numbers [24]. Whilst each of these papers give valuable insight into the heat transfer and flow phenomena, and develop increasing relevant models to those required by industry, they don't fully model the conditions or generate experimental data for the heat transfer distributions seen within an advanced turbine aerofoil leading edge cooling system. Often not combining the effects of a non-ideal concave target surface, non-ideal jet nozzle, or effects of an inclined jet.

Of note, this research is an expansion of one aspect of a larger investigation into the optimisation of cooling air usage in a double-wall structure previously introduced [25], with the aim to maximise the internal heat transfer enhancement, whilst considering the required cooling air. Fundamentally, this enhancement of heat transfer can generally be achieved in one of three ways: decreasing the boundary layer thickness, increasing the boundary layer turbulence, or decreasing the boundary layer viscosity. The viscosity is limited by the working fluid's properties and temperature, but the boundary layer thickness and turbulence are contributed to by several flow phenomena, and they are the focus of this study.

In this study, experimental and numerical techniques are utilised to investigate jet impingement cooling on a realistic leading edge region of a gas turbine blade geometry at a higher, more typical jet Reynolds number of up to 40,000. Experimental work relies primarily on data from a transient thermochromic liquid crystal (TLC) measurement technique at the target surface. To further investigate and understand the fluid flow and heat transfer within the geometry, and optimise cooling; a numerical study was conducted. This was undertaken with the same geometry using commercial computational fluid dynamics (CFD) software. The study was carried out with a row of five circular jets with the option of two target positions on the leading edge; A or B shown in Figure 1. A standard flat target plate impingement test was also experimentally conducted and compared against existing literature for method validation at identical geometry conditions.

Methods

Theoretical model

From the experimental testing, to create a useful dataset to industry, and to enable comparison against other research, the results are primarily in the format of non-dimensional value Nusselt Number (Nu) as a function of Re for various geometrical variations.

The Reynolds number is calculated based on the equation:

$$Re = \frac{\rho v l}{\mu} \quad (1)$$

Where density (ρ) is given by the fluid properties at the jet, velocity (v) is determined by the quantity of the mass flow rate calculated from the orifice plate's pressure drop as per ISO5167 [26]

, the characteristic length (l) is given by the jet's hydraulic diameter, and the dynamic viscosity of the fluid (μ) at the inlet conditions.

The Nusselt number for each point location is based primarily on the HTC data:

$$Nu = \frac{hl}{k} \quad (2)$$

Where the l is as above, the thermal conductivity (k) is based on the fluid properties at the inlet temperature, and the heat transfer coefficient (h) is calculated using the following method.

Past research [27] has shown that when a sudden temperature change is applied to a surface, transient one-dimensional conduction takes place within the assumed semi-infinite solid, meaning that Fourier's law can be applied, the general equation for this is shown:

$$\frac{\partial T}{\partial t} = \alpha \frac{\partial^2 T}{\partial x^2} \quad (3)$$

In our case we know the initial and boundary conditions:

$$t = 0 \quad (4)$$

$$T(x, 0) = T_i \quad (5)$$

$$x = 0 \quad (6)$$

$$-k \left(\frac{\partial T}{\partial x}\right) = h(T_\infty - T_w) \quad (7)$$

When the surface is then exposed to a fluid of constant temperature, HTC of h, and the initial temperature of the wall is considered unchanged as it effectively remains at an infinite distance from the surface.

$$x \to \infty \quad (8)$$

$$T(x,\mathrm{t}) = T_i \quad (9)$$

As previous research has shown [28], when the applied temperature has a sudden step change, the Fourier equation solves to:

$$\frac{T_w - T_i}{T_\infty - T_i} = 1 - exp(\beta^2)erfc(\beta) \quad (10)$$

Where:

$$\beta = h\sqrt{\frac{t}{\rho cpk}} \quad (11)$$

This however is only applicable where a step change is present, although all efforts have been made to induce as close to a step change in the incident temperature as possible, it is not practicable to make this exact.

Therefore the function is modified by Duhamel’s theorem, as previously utilised [29]:

$$T_w - T_i = \sum_{i=1}^{N} h(t-\tau_i)\Delta T_r \quad (12)$$

Where:

$$h(t-\tau_i) = 1 - exp\left(\frac{h^2}{k^2}\alpha(t-\tau_i)\right)erfc\left(\frac{h}{k}\sqrt{\alpha(t-\tau_i)}\right) \quad (13)$$

For this method to accurately gather HTC data for the test section, and following the semi-infinite wall assumption, all data must be gathered before the thermal pulse is transferred through the acrylic. For the 12mm minimum thickness acrylic used, this is calculated as 108 seconds, which is sufficient time for accurate transient results to be taken for the HTC.

To find the local values for temperature on the surface to use in this process, the hue of the liquid crystals is required. The TLC's optically active organic chemicals respond to heat, and a numerical scale can be placed on their hue colour bands from blue to red relative to a specified temperature increase, it is commonplace to select a single colour band to work with, with as linear relationship between hue red green blue colour and temperature is possible. In this work, the maximum green intensity method was used, as it is in the centre of the colour play, has a parabolic colour intensity relationship with temperature, and has an observable maximum green intensity, allowing the wall temperature to be monitored clearly by its relationship to a TLC hue value.

Experimental apparatus and procedure

The modular Perspex model shown assembled in Figure 2, within this diagram air flow can be followed from top left to bottom, through the subsections: Transition piece, main aerofoil passage plenum, jet impingement nozzle array (mainly obscured), leading edge target surface, expulsion to atmosphere. This is one variation of the test section that has been designed for use with air supply apparatus shown in Figure 3. This details the apparatus used to provide jet impingement of air against the leading edge target surface. The air blower supplies a constant mass flow of air, through the inline heat exchangers at a set air temperature. Pneumatic valves vent the air until a command is received to activate and direct the heated air towards the test section. The apparatus consists of a centripetal blower, an orifice flow meter, two inline heat exchangers, and two valves. The apparatus was designed to provide a step change in stable heated air supply to the test section as required. The test section serves as both the target heat transfer surface, and as the jet impingement nozzle arrangement. The modular design allows for variations in both jet and target configurations, of which those tested during this study are shown in Figure 4. This exploded diagram shows: 1 Transition piece, 2 Main aerofoil passage plenum, 3 Jet

Impingement nozzle row with sharp edge nozzles (for comparison with existing literature), 4 Jet Impingement nozzle row with realistic filleted nozzles, 5 Flat target surface (for comparison with existing literature), 6 Realistic leading edge concave target surface. 7-14 modular fixing equipment, 15 airtight gasket. The modules used in this study focus on a typical leading edge geometry that was developed in partnership with Siemens Industrial Turbomachinery Ltd. In preparation for the test, the blower speed is increased until the desired mass flow rate is achieved. The mass flow rate is obtained through the ISO5167 [26] procedure using a Furness FC0510 Micromanometer installed over the orifice plate, continuously monitoring the pressure differential at an accuracy of 0.25%. Using the method described by Kline and McClintock [30], the respective uncertainties of mass flow rate and Reynolds number are calculated as ±1.2% and ±1.5%. During testing heated air enters the test section when a fast action valves are activated. To match the engine conditions within a typical cooled blade; the supplied air flows into the impingement jets after turning a 90° angle towards the TLC coated target plate. The impingement jet configuration used in this test is an in-line array of 5 nozzles with radiused profile as shown in Figure 1. The jet temperature of each jet is measured using a calibrated thermocouple in a position at the inlet of each jet, the sample rate of which is 10 Hz. The target surface heat transfer is monitored with TLCs applied to the inside jet target surface and then coated in a black backing to give good contrast once they begin to display a colour change. The transient TLC colour change is recorded using Basler aca2040-90uc cameras, capable of 2040 px x 2046 px high resolution and 90 fps high speed recording. Total uncertainty for the Nusselt number based on the resolution of the camera, thermocouple, and data processing error is calculated at just over ±8%. Pressure measurements are taken at the inlet to the test section, before the jet nozzles, and after the jet nozzles.

As the primary focus of this study was to mimic typical industry leading edge geometries, the real manufacturing limitations between the two jet locations the dimensions were considered to represent two real possibilities, with the non-dimensional parameters in the region of; distance from the jet nozzle to the target surface $1.7 < H/D < 2.1$, the distance in x between subsequent jets, pitch $p/D = 4.4$, and concave target surface effective target diameter $C/D = 8.0$. Where D is the jet nozzle hydraulic diameter. H is calculated as the distance from jet nozzle exit to the impingement jet's target surface. p is the distance between centres of subsequent jets. Curvature (C) is an industry approximation of the target surface's concave diameter, used for reference against perfect semi-circular, concave target surfaces. In industrial design, the non-perfect curvature is often guided by requirements of external blade aerodynamic design, and material integrity driven wall thicknesses. Diagrammatical example of geometric parameters D, H, p, and C shown in Figure 5. The jet Reynolds number range covered during testing was 20,000 - 40,000.

A transient TLC method is used to analyse the time of maximum green intensity of the liquid crystals and therefore heat transfer coefficient of each test, with narrow band crystals from LCR-Hallcrest being applied (R36C01W) [31]. This method is based on the assumption of a one-dimensional conduction of the thermal pulse through the 'semi-infinite' plane wall of the 12mm Perspex target surface. These TLC's were calibrated through the Perspex to negate any effects of distortion or refraction during testing. The processing of the data is performed using a MATLAB script, which also uses a subtraction of the first reference image, from every subsequent image during testing, this removes any 'zero' imaging errors. The heat transfer coefficients are measured by timing the hue reaction of the TLC's against the time of this reaction, to further reduce error, a set hue value must be achieved for two consecutive frames in an effort to reduce any error caused by camera noise, or any other external influences such as fast-moving dust particles.

The experimental setup for this study was conducted with two variations of jet location (A and B), these are chosen because they impact the target surface in different ways and represent two possible primary variations in the aerofoil design, the relative locations of A and B can be seen in Figure 1.

A CFD analysis using Ansys CFX with the shear stress transport turbulence model was conducted and validated against the experimental data for target surface Nu. The domain is identical to that of the experimental testing in Figure 2, with walls at the initial air temperature (T≈293K), the outlets under identical atmospheric vent conditions (T≈333°C, P≈100,000 Pa), and the inlet using air of the same temperature (T≈333K), mass flow rate ($\dot{m}$≈0.1 kg/s), and turbulence intensity (I≈5%) as measured with hot-wire anemometry in the laboratory experiment. Boundary conditions, grid distribution, and model setup were guided by previous computational jet impingement studies [32]. These results for target Nu distribution are validated from the experimental data, and the fluid flow data is used to further analyse the flow and eddies within the leading edge geometry based on the jet's target location.

Results and discussion

The Nusselt number results obtained were validated against both Chupp et al. [18] and Cheng and Wang [33] for a similar Reynolds number of 10,000, and geometrical parameters of H/D and p/D; showing good agreement for a row of jets impinging on a concave target surface at those parameters.

To assess the effect of the jet location on the heat transfer coefficient, Nusselt number distributions across the target surface were generated for the parameter ranges of the present study. Results are generated for two jet location variations; A and B, at a jet Reynolds number range from 22,000 to 39,000.

The effects of jet location and Reynolds number on the target surface Nusselt number distribution are shown in Figure 6 - Figure 9. It is apparent in regions close to the sidewall that a plenitude of either very low Nusselt number, or very high Nusselt number specks exist, appearing as a grainy distribution. These specks are contributed to by both the air extraction around film holes located towards the blade walls appearing as increased local heat transfer, and a lack of TLC transition here. Inaccurate TLC transition is due to the local temperature not being sufficiently high to correctly activate the TLC within the time limits of the experiment. A higher jet temperature could improve the colour response in this region but would cause a faster, and less reliable response in the stagnation area and therefore lead to increased error in this region. As the stagnation region is the primary region of focus in this study we chose to concentrate data collection in this regions to the detriment of data in the sidewall region.

Figure 6 to Figure 9 show the effect of Reynolds number on Nusselt distribution for both jet location A and B, where all distributions show higher magnitudes of Nusselt number relative to Reynolds number, with similar Nusselt number distributions at both Reynolds numbers. Comparing the Nusselt number distributions relative to jet location, it is apparent that a higher relative magnitude is especially apparent in both the stagnation and fountain regions of jet location B.

It can be further observed from Figure 10 that Nu varies considerably between the five jets. Jets 1, 2, and 3 have similar trends and magnitudes of Nu irrespective of jet location or Re. The effects of nozzle inlet crossflow occur at jet 1, limiting the jet mass flow here. Slightly lower Nu is seen for subsequent jets; 4, and 5 then show a diminishing magnitude of Nu for all data sets, with especially pronounced decreases for jet location B. The factors affecting the diminishing Nu are primarily variations in the mass flow rate of each jet, and some nozzle crossflow effects.

The experimentally derived spanwise average distribution of Nu along the streamwise surface from $y/D = 0$ to 4.5 is shown in Figure 11, the locations of stagnation region are at $y/D = 1.25$ for jet location A, and $y/D = 2.25$. High local Nu data at the extremities of the test section; $0.5>y/D>4$ is due to the effect of film extraction holes in this region, and the speckles of inaccurately high or low HTC data, and does not give a true representation of surface HTC.

It can be further observed from Figure 11 that for both jet locations, when spanwise average Nusselt numbers are taken, the magnitude of Nu varies with Re. The effect of jet location however, has a significant impact on both the magnitude and trend of spanwise averaged Nu over the streamwise distribution. Spanwise Nu averages show higher Nu values for jet location A at 0.6<y/D<1.3, and for jet location B at 1.3<y/D<3.5.

A notable difference between the two Jet locations shown in Figure 11, for Jet location A the peak Nu is seen in the stagnation region, the Nu curve is highly symmetrical between 0.6<y/D<1.9. Due to the flow being constricted towards the 'suction side' of the blade at y/D=0; this symmetry isn't continued beyond y/D<0.6. Towards the 'pressure side' at 1.9<y/D<2.6 the Nu decreases lineally, this mild linear decrease may due to the boundary layer effect of decreased flow deceleration from the non-90° incident jet angle. At y/D = 2.6, a slight peak is observed at the location of the leading edge concave maxima. Between 2.6<y/D<3.6 the Nu remains almost consistent until the location of the 'pressure side' film holes at y/D = 4.

Figure 11 also shows that the spanwise averaged Nu over the streamwise distribution for jet location B has a less typical distribution. The stagnation region is observed at y/D = 2.25 to be symmetrical between 1.8<y/D<2.7, with significantly higher spanwise Nu average than the stagnation region of jet location A.

For the jets at location B at 2.7<y/D<3.5, the spanwise average Nu increases towards the film extraction holes, this is in part due to the high apparent heat transfer around these outlets, and partially due to the relatively high local Nu seen in the fountain regions of Figure 7 and Figure 9. From 0.6<y/D<1.8 an expected decrease of Nu is seen as the flow moves out of the stagnation region, this decrease shows a more typical logarithmic decrease than in jet location A and is due in part to the incident angle being at 90º to the target surface at the stagnation point.

The higher Nu values seen in jet location B are also contributed to in some capacity by the slightly larger H/D value compared to when the jet is in location A, but the contribution from each parameter be judged by varying the H/D and p/D values. To that end, correlations containing the specific target curvature effect on Nu can be produced. Based on the Nu distribution results, further analysis and variations can easily be validated and tested with numerical modelling.

With validation from the $\frac{Nu_0}{Nu_{ave}}$ experimental data and results from literature, the numerical model was built so that the flow phenomena related to each jet location can be observed.

From the CFD analysis, a side view of the average jet velocity in Jet location A can be seen in Figure 1, this also notes the two primary jet location variations. A specific look at the first Jet velocity in Jet location A can be seen in Figure 12. As expected, the highest velocity is seen at jet nozzle outlet, which then stagnates against the target surface, before turning 90 degrees towards the Y = 0 'suction side' and forming a large eddy throughout the concave cavity. Due to this eddy having a slower velocity than that caused in Jet location B, a larger boundary layer develops and leads to a lower heat transfer coefficient. The jet inlet velocity can be seen in Figure 13, and explains partially why jets 4 and 5 have a lower mass flow rate and therefore lower associated heat transfer coefficient.

Conclusions

The current experimental and numerical investigation was conducted into the flow and heat transfer characteristics of a typical turbine aerofoil geometry. TLC was used to gather a distribution of Nusselt number over the entire target surface and this was then compared against numerical data using commercial CFD techniques, allowing for further analysis of the internal flows. The primary focus of this testing was to analyse the effect of the jet's target location relative to the concave leading edge wall of a cooled gas turbine aerofoil at various jet Reynolds number values, specifically with a realistic target and nozzle geometry. The following conclusions are made:

1. At these geometry and fluid conditions, the location of highest local surface Nusselt number was seen in the jet stagnation point regardless of its location relative to the target geometry.
2. Mass flow and cross flow effects between the nozzles and target diminish the heat transfer effectiveness of each subsequent jet. Some effect is also experienced the inlet of the first jet nozzle, where there is an increased crossflow, causing a pressure reduction in the flow direction in the inlet manifold.
3. Jet row location B demonstrated larger Nusselt number values in almost all locations, compared to Jet location A.
4. Results show that the Nusselt number distribution is similar between the two jet locations with no notable differences in the distribution between jets other than with a particularly high Nusselt number seen in jet location B at the stagnation point and towards pressure side fountain regions.
5. Far more prominent crossflow swirl eddies are seen to develop in jet location A due to the non-90° incident jet angle, and how this angle reduces deceleration of the flow along the target surface compared to cases with the jets in location B.

Nomenclature

AM	Additive Manufacturing
CFD	Computational fluid dynamics
C	Effective diameter of concave target surface, m
cp	Specific heat, J/K.kg
D	Jet nozzle diameter, m

H Distance from jet nozzle to target surface, m

h Heat transfer coefficient, $Wm^{-2}K^{-1}$

HTC Heat transfer coefficient, $Wm^{-2}K^{-1}$

k Thermal conductivity, W/m.K

l Characteristic length, m

$\dot{m}$ Mass flow rate, kg/s

Nu Nusselt number

Nu_0 Stagnation point Nusselt number

Nu_{ave} Area average Nusselt number

P Pressure, Pa

p Pitch, or distance between jet nozzles in the x direction, m

Re Reynolds number

T Temperature, K

T_i Initial temperature, K

T_r Fluid mixed mean temperature, K

T_w Wall temperature, K

T_∞ Temperature at infinite distance, K

t Time, s

TLC Thermochromic liquid crystal

TET Turbine entry temperature, K

v Velocity, m/s

x Spanwise Direction, m

y Streamwise Direction, m

Greek Symbols

ρ Density, $^{kg}/_{m^3}$

α Thermal diffusivity, $^{m^2}/_{s}$

τ_i Time constant, s

μ Dynamic viscosity, pa.s

Acknowledgements

Thank you to Siemens Industrial Turbomachinery Ltd for continued funding, support and guidance in this project.

Acknowledgement is also due to support from the European Commission Research and Industry Staff Research and Innovation Staff Exchange (RISE) Thermasmart project.

References

[1] N. Zuckerman and N. Lior, “Jet Impingement Heat Transfer Physics, Correlations, and Numerical Modeling,” *Advances in Heat Transfer,* vol. 39, pp. 565-631. DOI:10.1016/S0065-2717(06)39006-5, 2006.

[2] R. K. Turton, Principles of Turbomachinery, London: Springer, 1994. DOI:10.1007/978-94-010-9689-8.

[3] J. C. Sanders and A. Mendelson, “Theoretical Evaluation of Methods of Cooling the Blades of Gas Turbines,” National Advisory Committee for Aeronautics. Lewis Flight Propulsion Lab, Cleveland, 1947.

[4] F. C. Yeh and F. S. Stepka, “Review and status of heat-transfer technology for internal passages of air-cooled turbine blades,” NASA Lewis Research Center, Cleveland, 1984.

[5] B. Lakshminarayana, “Turbine Cooling and Heat Transfer,” in *Fluid Dynamics and Heat Transfer of Turbomachinery*, Pennsylvania, John Wiley and Sons, Dec. 15 1995, pp. 597-721. DOI:10.1002/9780470172629.

[6] J.-C. Han, S. Dutta, and S. Ekkad, Gas Turbine Heat Transfer and Cooling Technology, Boca Raton: CRC Press, 2000. DOI:10.1201/b13616.

[7] J. L. Blackall, H. Iacovides, and J. C. Uribe, “Modeling of In-Line Tube Banks Inside Advanced Gas-Cooled Reactor Boilers,” *Heat Transfer Engineering,* vol. 41, no. 19-20, pp. 1731-1749, 2020. DOI:10.1080/01457632.2019.1640486.

[8] G. Chen, V. G. Gomes, and W. J. M. Douglas, “Impingement Drying of Paper,” *Drying Technology,* vol. 13, no. 5-7, pp. 1331-1344, 1995. DOI:10.1080/07373939508917025.

[9] L. F. G. Geers, M. J. Tummers, and K. Hanjalic, “Experimental investigation of impinging jet arrays,” *Experiments in Fluids,* vol. 36, no. 6, pp. 946-958, Jun. 2004. DOI:10.1007/s00348-004-0778-2.

[10] D. Cooper, J. D. C, B. E. Launder, and G. X. Liao, “Impinging jet studies for turbulence model assessment – I. Flow-field experiments,” *International Journal of Heat and Mass Transfer,* vol. 36, no. 10, pp. 2675-2684, Jul. 1993. DOI:10.1016/S0017-9310(05)80204-2.

[11] K. Kataoka, “Impingement heat transfer augmentation due to large scale eddies,” in *Proceedings of the 9th International Heat Transfer Conference*, Jerusalem, Aug. 19-24 1990. DOI:10.1615/IHTC9.1940.

[12] L. Huang and M. S. El-Genk, “Heat transfer of an impinging jet on a flat surface,” *International Journal of Heat and Mass Transfer,* vol. 37, no. 13, pp. 1915-1923, Sept. 1993. DOI:10.1016/0017-9310(94)90331-X.

[13] P. Gil and J. Wilk, “Heat transfer coefficients during the impingement cooling with the use of synthetic jet,” *International Journal of Thermal Sciences,* vol. 147, pp. 106-132, Jan. 2020. DOI:10.1016/j.ijthermalsci.2019.106132.

[14] J. W. Gregory and M. N. Tomac, “A Review of Fluidic Oscillator Development and Application for Flow Control,” in *AIAA 43rd Fluid Dynamics Conference*, San Diego, Jun. 24-27 2013.

[15] R. Gardon and J. C. Akfirat, “Heat Transfer Charecteristics of Impinging Two-Dimensional Air Jets,” *Journal of Heat Transfer,* vol. 8, no. 10, pp. 101-108, Oct. 1966. DOI:10.1016/0017-9310(65)90054-2.

[16] E. Sedighi, A. Mazloom, and A. Hakkaki-Fard, “Uniform Cooling of a Flat Surface by an Optimized Array of Turbulent Impinging Air Jets,” *Heat Transfer Engineering,* vol. 40, no. 20, pp. 1750-1761, Mar. 2019. DOI:10.1080/01457632.2018.1497123.

[17] A. W. Davis, J. Nillson, M. Osbourne, and C. Ravoux, “Testing of a gas turbine blade made by Selective Laser melting, in a gas turbine engine,” in *Proceedings of the 16th Heat Transfer Conference*, Nottingham, Sept. 8-10 2019.

[18] R. E. Chupp, H. E. Helms, P. W. McFadden, and T. R. Brown, “Evaluation of Internal Heat-Transfer Coefficients for Impingement-Cooled Turbine Airfoils,” *Journal of Aircraft,* vol. 6, no. 3, pp. 202-208, May/Jun. 1969. DOI:10.2514/3.44036.

[19] H. Martin, “Heat and Mass Transfer between Impinging Gas Jets and Solid Surfaces,” in *Advances in Heat Transfer,* vol. 13, Abingdon, Oxfordshire, Routledge, 1977. DOI:10.1016/S0065-2717(08)70221-1, pp. 1-60.

[20] L. Liu, X. Zhu, H. Liu, and Z. Du, “Effect of tangential jet impingement on blade leading edge impingement heat transfer,” *Applied Thermal Engineering,* vol. 130, pp. 1380-1390, Feb. 5 2018. DOI:10.1016/j.applthermaleng.2017.11.134.

[21] L. W. Florschuetz, C. R. Truman, and D. E. Metzger, “Streamwise Flow and Heat Transfer Distributions for Jet Array Impingement with Crossflow,” *Journal of Heat Transfer,* vol. 103, no. 2, pp. 337-342, May. 1981. DOI:10.1115/1.3244463.

[22] D. E. Metzger, T. Yamashita, and J. C. W, “Impingement Cooling of Concave Surfaces With Lines of Circular Air Jets,” *Journal of Engineering for Gas Turbines and Power,* vol. 91, no. 3, pp. 149-155, Jul. 1969. DOI:10.1115/1.3574713.

[23] R. Pearce, P. Ireland, E. Dane, and J. Telisinghe, “A Comparison of Experimental and Computational Heat Transfer Results for a Leading Edge Impingement System,” *International Journal of Turbomachinery Propulsion and Power,* vol. 3, no. 4, p. 23, Nov. 2018. DOI:10.3390/ijtpp3040023.

[24] V. S. Patil and R. P. Vedula, “Local heat transfer for jet impingement onto a concave surface including injection nozzle length to diameter and curvature ratio effects,” *Experimental Thermal and Fluid Science,* vol. 92, pp. 375-389, Apr. 2018. DOI:10.1016/j.expthermflusci.2017.08.002.

[25] E. Wright, A. Ahmed, Y. Yan, J. Maltson, and L. Arisso Lopez, “Experimental and Numerical Heat Transfer Investigation of Impingement Jet Nozzle Position in Concave Double-Wall Cooling Structures,” in *Proceedings of the 16th UK Heat Transfer Conference*, Nottingham, Sept. 8-10 2019.

[26] I. O. f. Standardisation, “ISO5167-2 Measurement of fluid flow by means of pressure differential devices inserted in circular-cross section conduits funning full,” International Organisation for Standardisation, Geneva, 2003.

[27] F. P. Incropera, D. P. Dewitt, T. L. Bergman, and A. S. Lavine, Fundamentals of Heat and Mass Transfer, Hoboken: John Wiley and Sons, 2007.

[28] T. V. Jones, S. T. Dunne, and R. J. Clifford, “Techniques for obtaining detailed heat transfer coefficient measurements within gas turbine blade and vane cooling passages,” in *International Gas Turbine Conference and Exhibit*, Phoenix, Mar. 27-31 1983.

[29] D. E. Metzger and D. E. Larson, “Use of Melting Point Surface Coatings for Local Convection Heat Transfer Measurements in Rectangular Channel Flows With 90-deg Turns,” *Journal of Heat Transfer of The American Society of Mechanical Engineers,* vol. 108, no. 1, pp. 48-54, Feb. 1986. DOI:10.1115/1.3246903.

[30] S. J. Kline and F. A. McClintock, “Describing uncertainties in single sample experiments,” *Mechanical Engineering,* vol. 75, no. 1, pp. 3-8, 1953.

[31] LCRHallcrest, “Handbook of Thermochromic Liquid Crystal Technology,” LCRHallcrest, Glenview, Illinois, 2015.

[32] A. Dewan, R. Dutta, and B. Srinivasan, “Recent Trends in Computation of Turbulent Jet Impingement Heat Transfer,” *Heat Transfer Engineering,* vol. 33, no. 4-5, pp. 447-460, Nov. 2011. DOI:10.1080/01457632.2012.614154.

[33] J.-R. Cheng and B.-G. Wang, “Experimental Investigation of Heat Transfer by a Single and a Triple-Row Round Jets Impinging on Semi-Cylindrical Concave Surfaces,” in *International Heat Transfer Conference,* Munich, Sept. 6-10 1982. DOI:10.1615/IHTC7.1940.

Figures

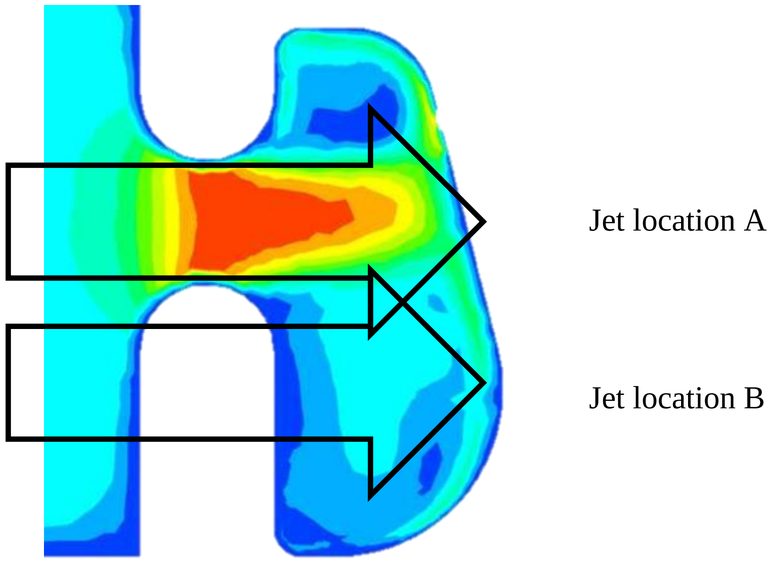

Figure 1 – Example of numerical average jet centreline velocity distribution with indicated arrows showing direction and location of nozzle flow for jet locations A and B.

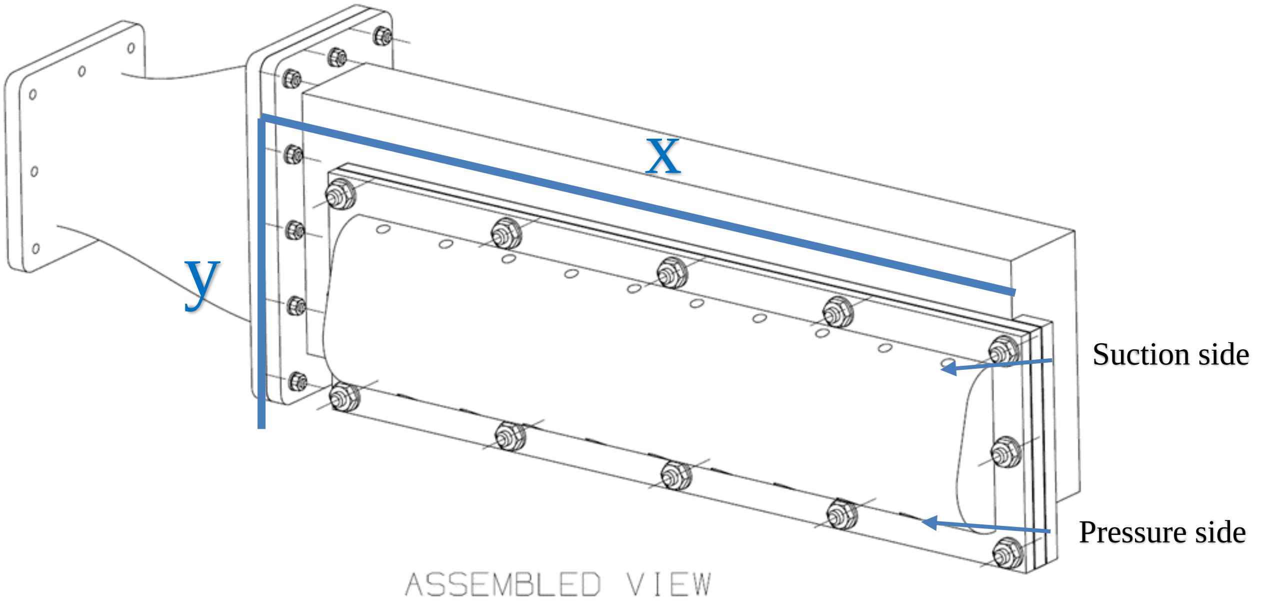

Figure 2 – View of assembled test section showing coordinate reference system.

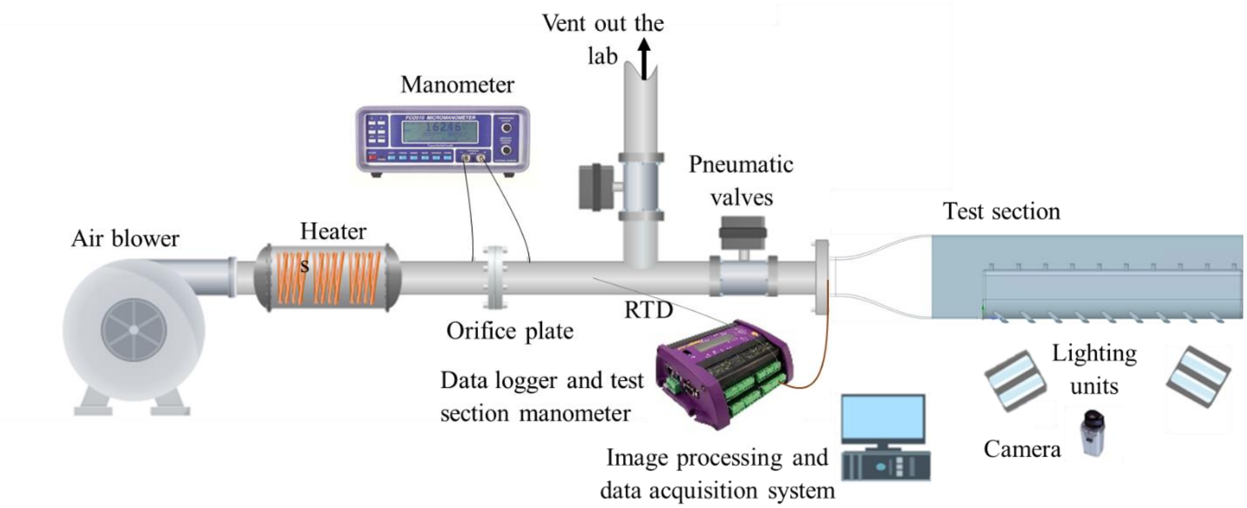

Figure 3 – Schematic diagram of experimental setup and data collection apparatus.

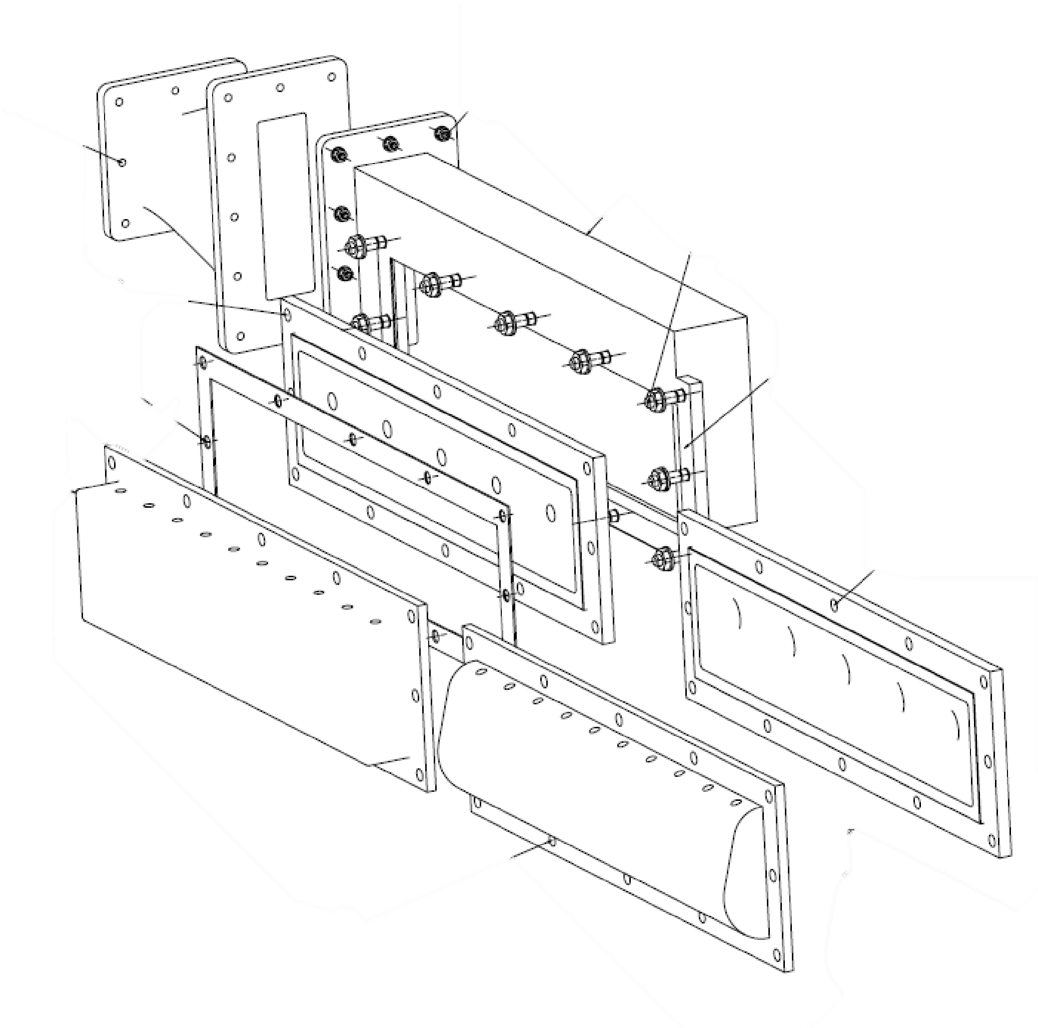

Figure 4 – View of exploded test section.

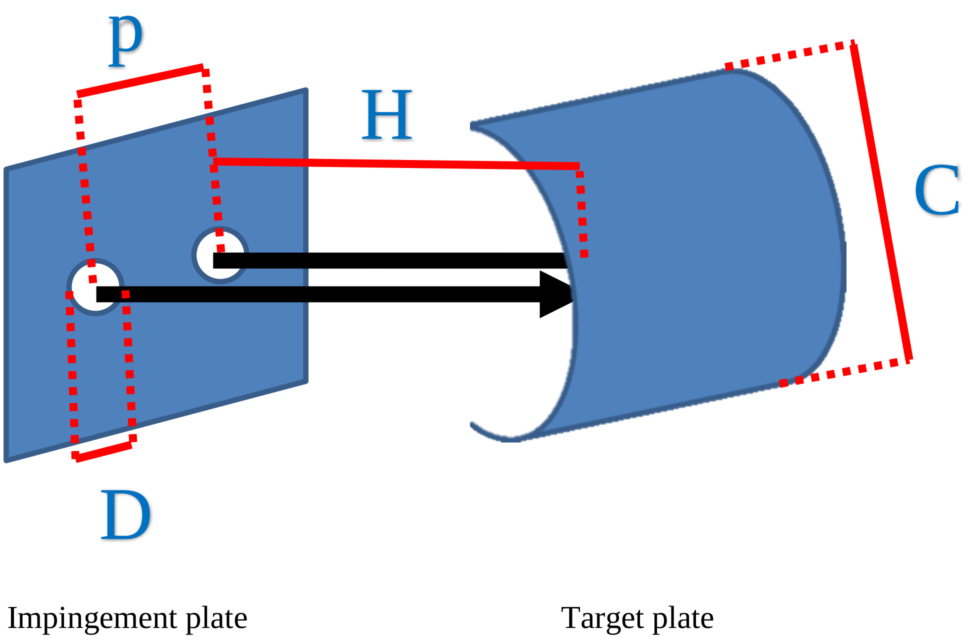

Figure 5 – Example diagram of key geometric parameters

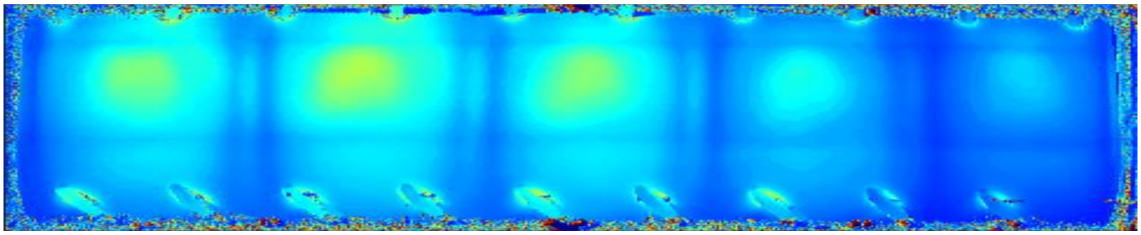

Figure 6 – Target surface Nusselt number distribution for jet location A at 22,000 Re.

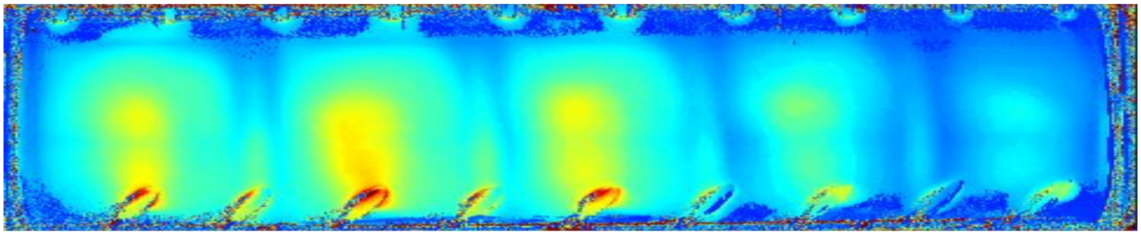

Figure 7 – Target surface Nusselt number distribution for jet location B at 22,000 Re

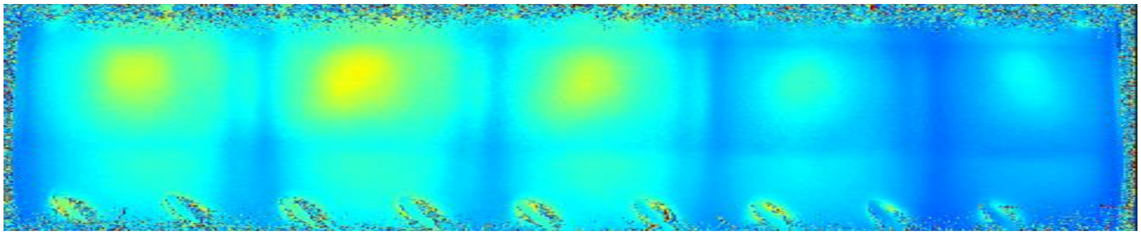

Figure 8 – Target surface Nusselt number distribution for jet location A at 39,000 Re

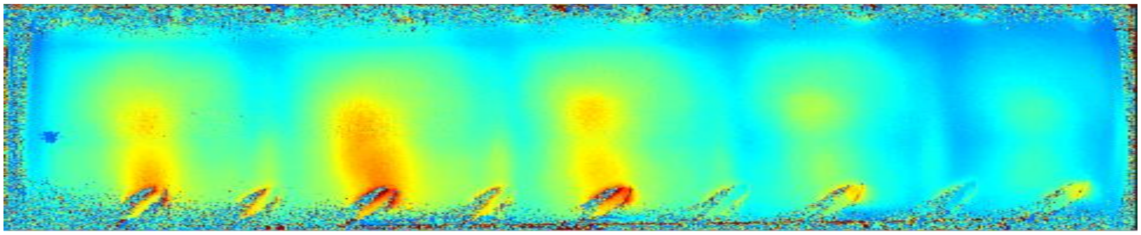

Figure 9 – Target surface Nusselt number distribution for jet location B at 39,000 Re

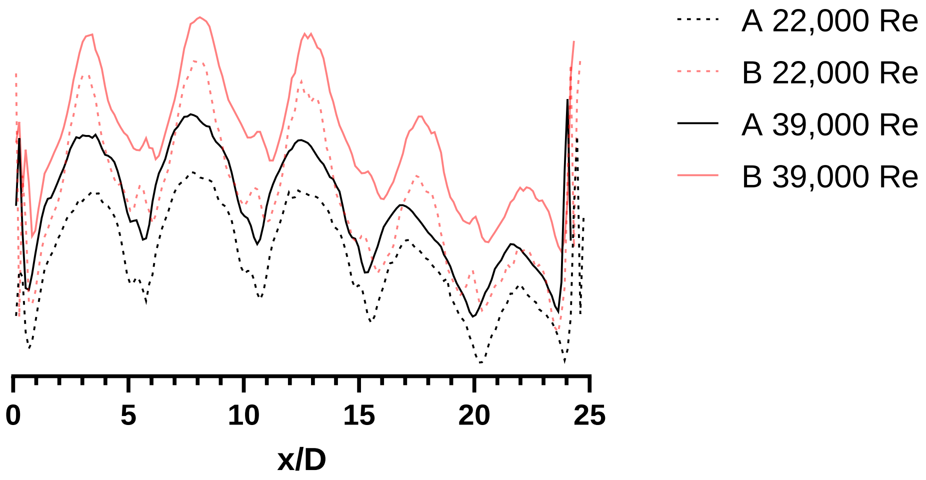

Figure 10 - Effects of jet location and Reynolds number on streamwise averaged Nusselt number from y/D = 0 at 'aerofoil hub' cooling passage inlet.

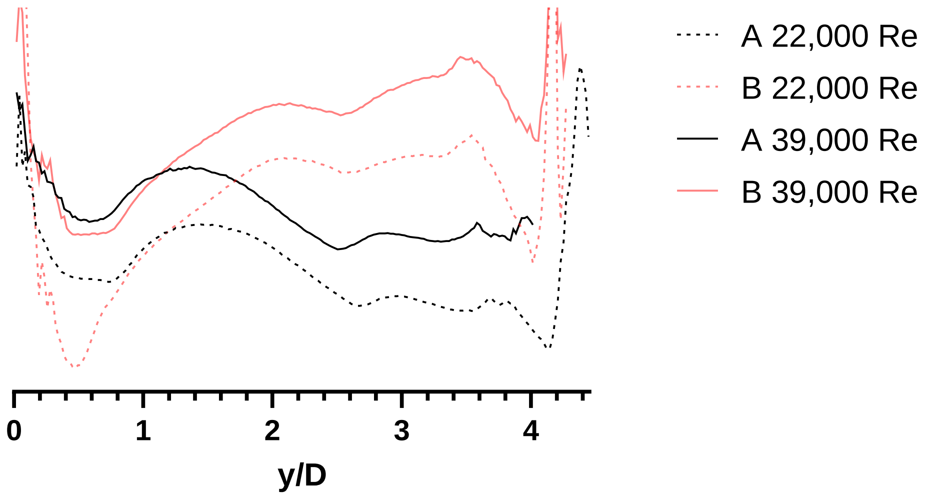

Figure 11 - Effects of jet location and Reynolds number on spanwise averaged Nusselt number from y/D = 0 at 'suction side' wall.

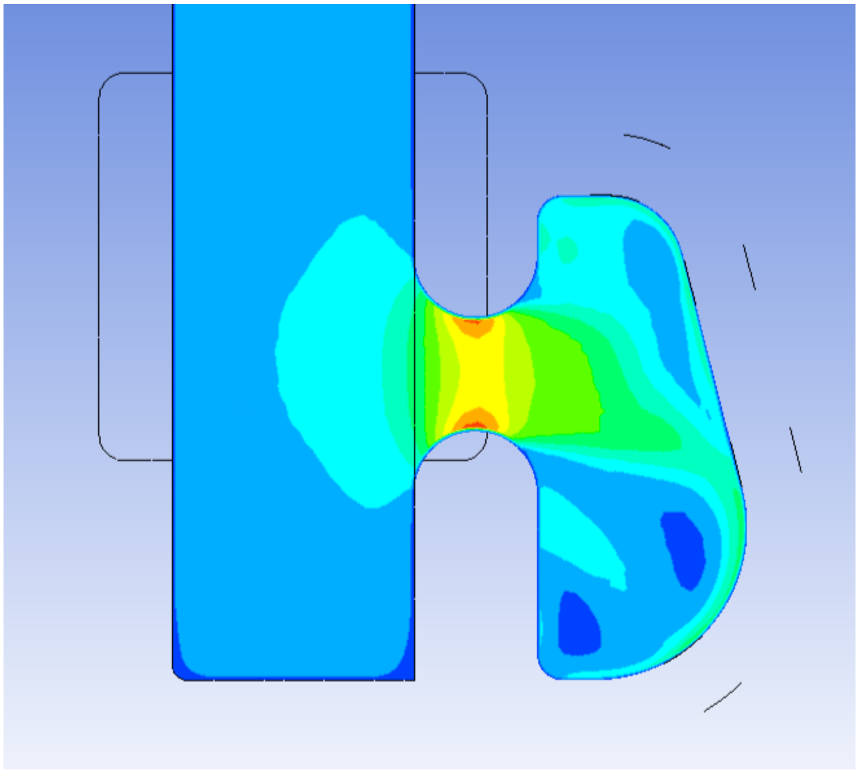

Figure 12 – Numerical velocity distribution though jet nozzle 1 centreline in jet location A.

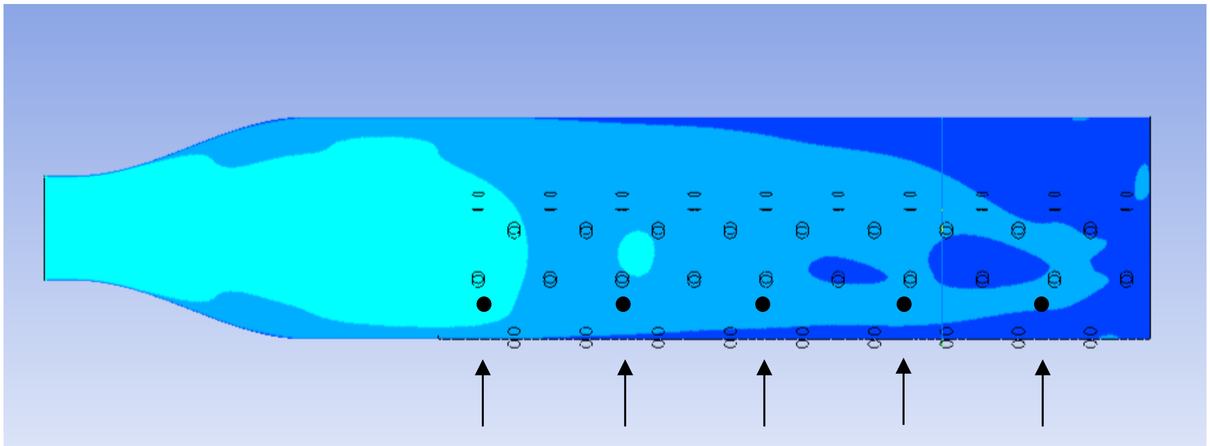

Figure 13 - Numerical velocity distribution though jet nozzle through aerofoil passage plenum centreline. Black markers indicating the spanwise position of jets 1 through 5 (from left to right), at their exact position marked by black dots.

Notes on contributors

Edward Wright is a PhD student within the Fluids and Thermal Engineering Research Group of the University of Nottingham. He obtained his MEng from the University of Lincoln, being partnered with Siemens Industrial Turbomachinery Ltd, in Lincoln since 2013. He has worked closely with industry, helping to improve processes and technology to create an improved product. Notable collaboration with Siemens includes three University projects related to the cooling of hot end turbine components. He is currently using experimental and numerical methods to determine heat transfer properties and the nature of fluid flow within high temperature turbine aerofoil components, primarily investigating jet impingement and film cooling.

Abdallah Ahmed is a third year PhD student in the Department of Mechanical, Materials, and Manufacturing Engineering at the University of Nottingham, United

Kingdom. His doctoral research investigates the use of reverse jet impingement as a new double-wall cooling technique to enhance the heat transfer rate by increasing the internal surface area without noteworthy pressure drop. He uses a multidisciplinary heat transfer approaches that encompasses the transient liquid crystal technique in the experimental work and the computational fluid dynamics technique in the numerical work. He holds a bachelor's degree and master's degree in Mechanical Power Engineering from Cairo University, Egypt.

Yuying Yan is a Professor and Chair in Thermofluids Engineering in Faculty of Engineering at University of Nottingham, UK. He obtained BSc in 1982 at Jilin University, MSc in 1986 at Shanghai Institute of Mechanical Engineering and Ph.D. in 1996 at City University of London. He started his academic position in the UK at Nottingham Trent University since 1998 after survived two years as Research Fellow in Chemical & Process Engineering at University of Surrey. He has joined the University of Nottingham since 2004. His research covers widely ranged area of flow and heat transfer including heat transfer enhancement, phase changes, surface wetting, nanofluids and nature inspired solutions and energy efficiency, as well as energy storage and thermal management.

**John Maltson** received his PhD from Coventry, and his degree in Mechanical Engineering from Trent, Nottingham. He has over thirty years of experience in gas turbine cooling, heat transfer, fluid flows, and transient thermal analysis. He has been the author or co-author of several conference and journal papers and has had a few patent applications granted.

**Lynda Arisso Lopez** was a student researcher in the Fluids and Thermal Engineering Research Group at the University of Nottingham in 2019. She obtained her MSc in Energy Conversion and Management at University of Nottingham in 2019. She developed a research investigation to study novel aerodynamic geometries to improve the cooling effectiveness on turbine blades and nozzles. She has over five years of experience in the Sustainable Energy field. She is Design Manager of Solar at Infinis-Solar from June 2020.